CONF-8106[illegible]-7

LA-UR -81-1936

TITLE: TWO-DIMENSIONAL THEORY AND SIMULATION OF FREE-ELECTRON LASERS

AUTHOR(S): Thomas J. T. Kwan and J. R. Cary

MASTER

SUBMITTED TO: 4th International Topical Conference on High-Power Electron and Ion-Beam Research and Technology
Palaiseau, France
June 29 - June 3, 1981



University of California

LOS ALAMOS SCIENTIFIC LABORATORY
Post Office Box 1663 Los Alamos, New Mexico 87545
An Affirmative Action/Equal Opportunity Employer

Form No. 836 R3
St. No. 2629
12/78

UNITED STATES
DEPARTMENT OF ENERGY
CONTRACT W 7405-ENG 36



ED6

# TWO-DIMENSIONAL THEORY AND SIMULATION OF FREE ELECTRON LASERS*

Thomas J. T. Kwan and John R. Cary**
Applied Theoretical Physics Division
Los Alamos National Laboratory
Los Alamos, New Mexico, USA 87545

## ABSTRACT

Two-dimensional homogeneous theory of free-electron lasers with a wiggler magnetic field of constant wavelength is formulated. It has been found from the theory that waves propagating obliquely with respect to the electron beam are always unstable with appreciable growth rates; therefore, mode competition among the on-axis and off-axis modes is an important consideration in the design of the free-electron laser. Furthermore, electromagnetic waves with group velocities opposite to the direction of electron beam propagation are absolutely unstable if $k_o v_o > \omega_{pe}(1/\gamma^{3/2} + 1/\gamma^{1/2})$. Due to strong nonlinear saturation levels of the low-frequency absolute instability, the dynamics of the electron beam and the generation of the high-frequency electromagnetic radiation can be severely affected. Two-dimensional particle simulations show that the efficiency of generation of the on-axis high-frequency electromagnetic wave decreases significantly due to instability of the off-axis modes. In addition, complete disruption of the electron beam and laser oscillation due to the onset of the absolute instability have been observed in simulations.

## INTRODUCTION

Generation of coherent electromagnetic radiation by relativistic electron beams has been under intensive theoretical and experimental studies in recent years. In particular, the concept of free-electron laser, which is a scheme of generating tunable coherent radiation based on the interaction between a relativistic electron beam and a static periodic magnetic field, has attracted enormous attention in the scientific community. The very attractive fundamental characteristics of the free-electron laser are tunability, high power, and high efficiency in the production of electromagnetic radiation.

There has been a considerable amount of theoretical and numerical investigation of the free-electron laser using a one-dimensional model (1). In the one-dimensional model, the wavelength of the radiation is given by $\lambda = \lambda_o(1 - \beta)/\beta \simeq \lambda_o/2\gamma^2$ where $\lambda_o$ and $v_o$ are the wavelength of the wiggler field and the velocity of the electron beam, respectively.

*This work was supported by the U.S. Department of Energy.

**Present address Institute for Fusion Studies, University of Texas.

However, the free-electron laser can, in general, produce radiation that propagates at an angle to the electron beam (2) as long as the resonance condition, $\omega = (k\cos\theta + k_o)v_o$, is satisfied. This imples that radiation with frequency $\omega = k_o v_o/(1 - v_o\cos\theta/c)$ can be amplified and the free-electron laser can be a very broad band simplifier.

## TWO-DIMENSIONAL DISPERSION RELATION OF FREE-ELECTRON LASERS

We consider an electron beam moving through a static periodic magnetic field which is given by

$$\vec{B}_o = \delta B_o(\hat{e}_x \cos k_o z + \hat{e}_y \sin k_o z) \quad . \tag{1}$$

where $\delta B_o$ measures the strength of the static magnetic field and $k_o = 2\pi/\lambda_o$ is the wavenumber. We assume that the electron beam is charge and current neutralized on average by a massive background of ions. We also assume that the electron is monoenergetic with total energy $\gamma_o mc^2$ and an average velocity in the z-direction.

The self-consistent equilibrium of the electron beam due to this static periodic magnetic field can be found by solving the equation of motion and Maxwell's equations. The self-consistent momentum of the electron beam is given by

$$\vec{p}_o = (\gamma_o^2 - \omega_{ce}^2 k_o^2/\kappa^4 c^2 - 1)^{\frac{1}{2}} \hat{e}_z - m_o \omega_{ce} k_o \kappa^{-2} (\hat{e}_x \cos k_o z + \hat{e}_y \sin k_o z), \tag{2}$$

where $\kappa^2 = k_o^2 + \omega_{pe}^2/\gamma_o c^2$, and $\omega_{pe} = (4\pi e^2 n_o/m_o)^{\frac{1}{2}}$ and $\omega_{ce} = e\delta B/m_o c$ are the electron plasma frequency and the electron cyclotron frequency, respectively. The total magnetic field, which is the sum of the external field and the diamagnetic field of the electron beam, is given by

$$\vec{B} = (1 - \omega_{pe}^2/\gamma_o \kappa^2 c^2)\, \delta B_o\, (\hat{e}_x \cos k_o z + \hat{e}_y \sin k_o z). \tag{3}$$

Since the static periodic magnetic field in the laboratory frame, as given by Eq. (1), is a traveling electromagnetic wave in the frame of the electron beam, it obeys the dispersion relation

$$\omega_c = -k_o' v_o \quad , \tag{4}$$

where $\omega_o'$ and $k_o'$ are the frequency and wavenumber of the static magnetic field in the beam frame and $v_o$ is the axial velocity of the electron beam. Hence, in the beam frame, the physical process of free electron lasers is equivalent to that of stimulated scattering of electromagnetic waves in a plasma. The dispersion relation of the scattering process is well known and was derived by Drake et al.(2) and Mannheimer and Ott.(3) By applying a Lorentz transformation to the dispersion relation, we obtain the two-dimensional dispersion relation of free-electron lasers in the laboratory frame as follows:

$$[\omega - (k_z + k_o)v_o]^2 - \frac{\omega_{pe}^2}{\gamma_z^3}\left(\omega^2 - k^2c^2 - \frac{\omega_{pe}^2}{\gamma_z}\right) = \frac{\omega_{pe}^2\,\omega_{ce}^2}{4\gamma_z^3\,k_o^2}\left(1 + \frac{\omega_{pe}^2}{\gamma_z\kappa^2c^2}\right)^2$$

$$\times \frac{[k_x^2 + \gamma_z^2(k_z + k_o - \omega v_o/c)^2]\,[k_x^2 + 2\gamma_z^2(k_z - \omega v_o/c^2)^2]}{[k_x^2 + \gamma_z^2\,(k_z - \omega v_o/c^2)^2]}\,, \qquad (5)$$

where $\gamma_z = (1 - v_{oz}^2/c^2)^{-\frac{1}{2}}$. Note that we are using rectangular geometry in which all physical quantities vary with z and x and are independent of y. The dispersion relation in Eq. (5) clearly shows the mode-coupling characteristics. On the left-hand side of Eq. (5) are the electromagnetic and electrostatic dispersion relations, which are coupled by the expression on the right-hand side. The coupling term is proportional to the second power of the strength of the static periodic magnetic field. Using the dispersion relation, one can analyze the free-electron laser instability in two dimensions. However, an analytical expression for the growth rate is difficult to obtain in the general case, and numerical analysis is, therefore, most suitable. One can rewrite the dispersion relation as a sixth order polynomial in $\omega$, which can be readily solved numerically in a computer. In Fig. 1 we present the contour plot of the temporal growth rates in $k_x$ and $k_z$. The contours of the growth rate are symmetric with respect to the $k_z$ axis. The parameters used in the computation are $\omega_{ce}/\omega_{pe} = 1.58$, $k_o c/\omega_{pe} = \pi$, and $\gamma_o = 1.6$. Note that the scale of the two axes are different, and the contours are centered around a rather flat and skinny elipse where crossings of the beam modes and the electromagnetic modes occur. If the condition $k_o v_o > \omega_{pe}(1/\gamma^{3/2} + 1/\gamma^{1/2})$ is satisfied, the resonant ellipse encloses the origin; and electromagnetic waves at all angles are unstable. The frequency range which is proportional to $\gamma_o^2$ can

be very broad. Furthermore, electromagnetic waves with group velocities opposite to the beam volocity are absolutely unstable.

## RESULTS FROM COMPUTER SIMULATION

The simulation results presented here were obtained from a modified version of CCUBE (4), which is a two-and-one-half-dimensional fully electromagnetic, relativistic, particle-in-cell, plasma simulation code. In the simulation of free-electron lasers, a relativistic electron beam with a specified energy, $\gamma_o mc^2$, is injected into the system. Charge and current neutralization of the electron beam were obtained through the use of immobile background ions in the simulations. The electron beam is subjected to the external magnetic field given in Eq. (1).

In Fig. 2 we show the phase space ($p_z$ vs z) of the electron beam at $T = 45\ \omega_{pe}^{-1}$ in a simulation. The parameters of the simulations were $\gamma_o = 1.6$, $k_o c/\omega_{pe} = \pi$, and $\omega_{ce}/\omega_{pe} = 1.58$. It is evident from Fig. 2 that a low-frequency electrostatic wave, coupled with a backward electromagnetic wave, had grown to considerable amplitude to start trapping the electron beam. This electrostatic wave had a well-defined longitudinal wavelength, which was measured to be approximately $2.47\ \omega_{pe}^{-1}$. Figure 2 also shows the existence of short wavelength (high-frequency) waves, which were trying to grow at the same time as the low-frequency wave.

One component of the electromagnetic field at a particular axial position is shown as a function of x in Fig. 3 , which clearly shows that the perpendicular perturbation had two wavelengths (mode two). One should note that the number of wavelengths in the perpendicular direction had to be an integer because periodic boundary conditions were used in that direction in the simulation. As indicated in Fig. 3, the perpendicular wavelength was approximately $7.0\ c\omega_{pe}^{-1}$. Therefore, the angles of propagation of the electrostatic and the electromagnetic waves were abou. 20° and 128°, respectively. The absolutely unstable low-frequency waves eventually grew to the point where they totally disrupted the electron beam and thus the generation of the high-frequency radiation. The time history and its Fourier transform of the electromagnetic field at a fixed position near the entrance of the system is shown in Fig. 4, which clearly illustrates the onset of the low-frequency absolute instability. The frequency of the unstable wave measured from Fig. 4 was $\omega \approx 1.23\ \omega_{pe}$. The frequency, longitudinal and perpendicular wavelengths, and angle of propagation of the absolutely unstable wave obtained from the simulation agree with the theoretical results well within 10%.

Finally, we show the temporal growth rates as a function of angles of propagation in Fig. 5. The growth rates were obtained by the numerical pinch-point analysis (5) of the dispersion relation in Eq. (5). The physical parameters are the same as in the simulation. The growth rate increases rapidly from $\theta = 90^\circ$ and flattens out after $\theta = 120^\circ$. Our numerical evaluation indicates that mode three or higher in the perpendicular direction corresponds to waves propagating at an angle of $105^\circ$ or smaller, and they have substantially smaller growth rates than modes one and two. Therefore, one would expect that waves corresponding to higher mode numbers in the perpendicular direction would be dominated by modes one and two in the simulation. The fact that mode two was the only dominant mode observed in the simulation was probably due to the uneven level of the noise spectrum which existed in the simulation.

The dispersion relation in Eq. (5) predicts growth of off-axis electromagnetic waves in free-electron lasers. One of the effective ways to study the instability of the off-axis modes in a computer simulation is to launch a particular off-axis electromagnetic wave and to observe its amplification as it propagates and interacts with the electron beam. The boundary conditions of simulation are periodic in x and absorptive in z for both particles and fields. Due to the periodicity in x, the wavenumbers of the waves in the perpendicular direction ($k_x$) in the simulation were quantized; i.e., $k_x = 2\pi n/L_x$, where n is an arbitrary integer and $L_x$ is the length of the system in the perpendicular direction. The arbitrary integer, n, is limited by the resolution of short wavelength waves in a particular simulation. In our simulation, mode eight (n = 8) in the perpendicular direction is the shortest wavelength which can still be accurately resolved.

An off-axis electromagnetic wave was launched in our simulation with $n = 6$ ($k_x = 2\pi n/L = 2.69\ c^{-1}\omega_{pe}$) and $\theta = 40.0^\circ$, which is the angle between the directions of the wave and the electron beam propagation. The initial amplitude of the wave was $eE_o/m_o c\omega_{pe} = 0.08$, which corresponded to a power density of 4.35 $MW/cm^2$. In Fig. 6, we show the electric component of the electromagnetic wave as a function of the axial distance at a fixed perpendicular position at $\omega_{pe}t = 22.0$. The dots in Fig. 6 are data obtained from the simulation, and the solid curve is obtained by a least squares fit of the data. The axial wavenumber is found to be $k_z = 2.96\ c^{-1}\omega_{pe}$, and this wave is a mode six ($k_x = 2.69\ c^{-1}\omega_{pe}$) in the perpendicular direction as expected. The angle at which the wave propagates with respect to the electron beam is given by $\theta = \tan^{-1}(k_x/k_z) = 42.3^\circ$, which agrees quite well with the theoretically predicted value of

40.0°. From the variation of the wave amplitude along the axial position, we obtained a convective growth rate of $Im(k_z) = 0.265\ c^{-1}\omega_{pe}$ which is about 10% smaller than the theoretical value given by the dispersion relation in Eq. (5). The small discrepancy is probably due to collisional damping in the simulation and the cold fluid approximation used in obtaining the dispersion relation.

Significant modifications of the results from the previous analysis and computer simulations are expected to occur when finite boundary conditions are taken into account. When the sides of the resonant cavity are transparent or absorbing, the production of off axis modes should be poor since the waves leave the gain region before any significant amplification. On the other hand, incidental reflecting surfaces can lead to excitation of parasitic modes. As far as absolute instabilities are concerned, only the purely backward wave should be important for resonant cavity with transparent or absorbing walls. Furthermore, the absolute instability of the purely backward mode can be suppressed if the length of the region is less than the critical length (6) defined by

$$L_c = \pi |v_{g1} v_{g2}|^{1/2} / 2\,Im(\omega) \qquad (6)$$

where $v_{g1}$ and $v_{g2}$ are the group velocities of the two modes, and $Im(\omega)$ is the infinite medium growth rate.

## CONCLUSION

We have investigated the production of off-axis modes and absolute instability in free-electron lasers. We found that parasitic modes and absolute instabilities can exist in free-electron lasers and these modes can potentially affect its performance in producing coherent high-frequency electromagnetic radiation. However, we also discovered that one can minimize the effects by imposing proper constraints in the design of the free-electron laser cavity.

## REFERENCES

1. There is a large amount of published work in this area; for example, F. A. Hopf, P. Meystre, M. O. Scully, and W. H. Louisell, Phys. Rev. Lett. 37, 1342 (1976); T. Kwan, J. M. Dawson, and A. T. Lin, Phys. Fluids 20, 581 (1977); P. Sprangle, Cha-Mai Tang, and W. M. Manheimer, Phys. Rev. A 21, 301 (1980).

2. J. F. Drake, P. K. Kaw, Y. C. Lee, G. Schmidt, C. S. Lui, and M. N. Rosenbluth, Phys. Fluids 17, 778 (1974).

3. Wallace M. Manheimer and Edward Ott, Phys. Fluids 17, 1413 (1974).

4. B. B. Godfrey, in Proceedings of the 8th Conference on Numerical Simulation of Plasmas, June 28-30, 1978, Monterey, California., PE-3.

5. Richard J. Briggs, Electron-Beam Interaction with Plasmas, (MIT Press, Cambridge, Mass., 1964) Chapter 2.

6. D. Pesme, G. Laval, and R. Pellat, Phys. Rev. Lett. 31, 203 (1973).

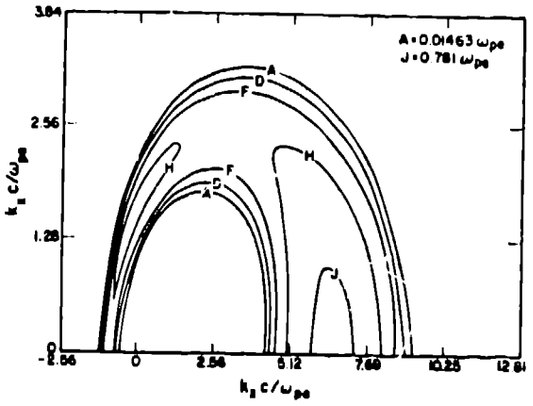


Fig. 1

Contours of growth rates of the free-electron laser in two dimensions centered around the resonant ellipse.

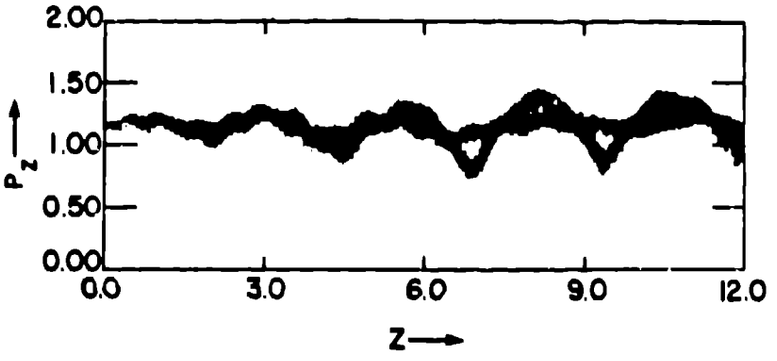


Fig. 2

Phase space diagram ($p_z$ vs z) of the electron beam $\omega_{pe}t$ = 42.41. The long wavelength modulation was due to the low-frequency absolute instability, and the short wavelength perturbations were due to the high-frequency convective instability.

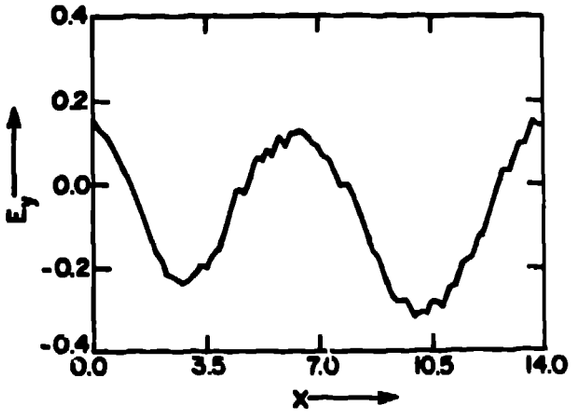


Fig. 3

Simulation showed that the high-frequency electromagnetic wave had two wavelengths in the perpendicular direction.

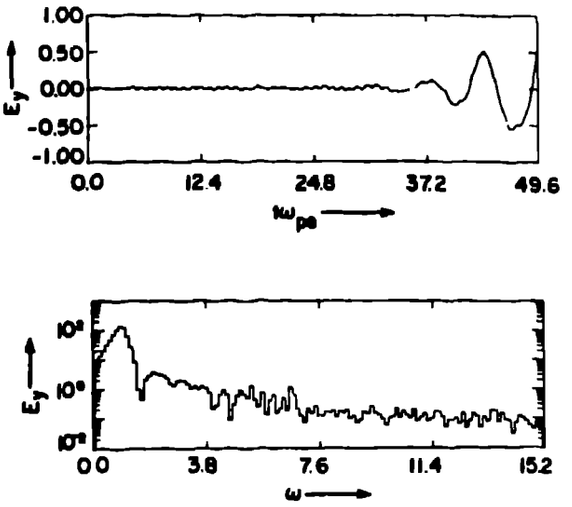


Fig. 4

The time history and the Fourier transform of the electromagnetic field. The onset of the absolute instability is clearly demonstrated.

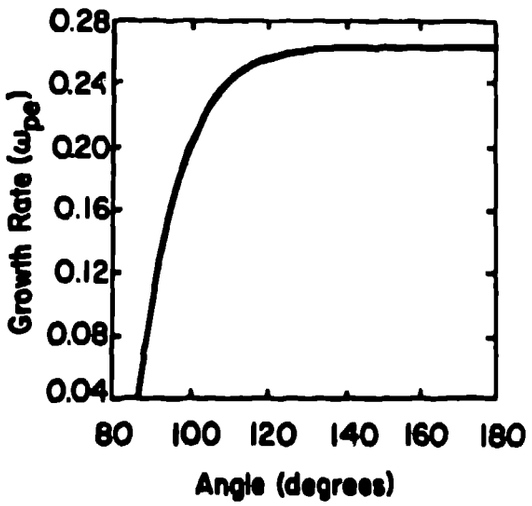


Fig. 5

Temporal growth rates as a function of angles as obtained by numerical pinch point analysis of the two-dimensional dispersion relation.

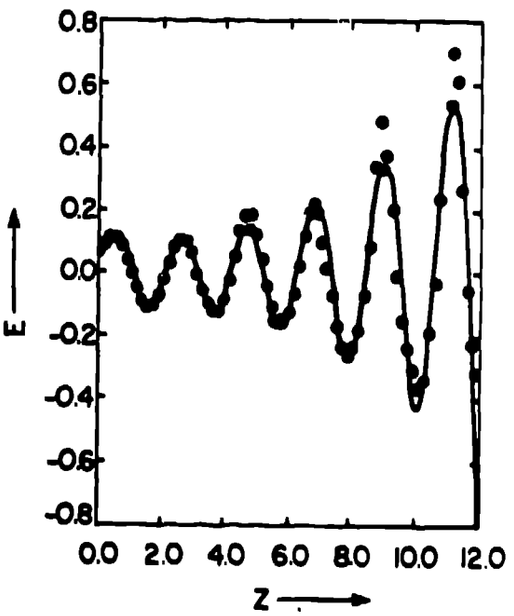


Fig. 6

Amplification of an off-axis electromagnetic wave in a computer simulation. The solid line is the least square fit of the data obtained from the simulation.